JOURNAL OF THEORETICAL
AND APPLIED MECHANICS
49, 3, pp. 665-683, Warsaw 2011

MODEL UPDATING IN STRUCTURAL DYNAMICS THROUGH A CONFLUENCE ALGORITHM

Maria Chierichetti
Massimo Ruzzene
Georgia Institute of Technology, School of Aerospace Engineering, Atlanta, USA
e-mail: mchierichetti@gatech.edu; massimo.ruzzene@aerospace.gatech.edu

The identification of the dynamic response of a structure in the presence of structural degradation has potential practical use on health monitoring systems and can contribute to improve the safety of rotorcraft flight and wind-turbine operations and to decrease their handling costs. A combined numerical and experimental procedure, called *Property Identification Algorithm*, updates the numerical model based on a limited set of experimental measurements in order to accurately predict the dynamic response of a system in the presence of structural degradations. The algorithm is designed based on modal decomposition and discrete experimental measurements, and is formulated in the case of periodic excitations. It is demonstrated that the updated dynamic response represents an accurate map of the experimental response in the domain. The paper describes the proposed algorithm and presents validation cases.

Key word: displacement mapping, inverse problem, FEM, experimental update, modal expansion

1. Introduction

The ability to assess the effects of changes in the physical properties of a structure from experimental measurements is crucial for understanding its real dynamic behavior because of the possible improvements in the maintenance of critical dynamic components connected to it. Modifications in mass and stiffness affect the performance of the system and can result in an increase of the vibrations of the structure and in higher fatigue loads. Therefore, the accurate prediction of the vibration levels of a system could result in improvements of Condition Based Maintenance processes.

Wind turbines and helicopter blades are particularly affected by this problem. Icing (Fig. 1a) and accumulation of dirt and bugs (Fig. 1b) significantly affect the maintenance of wind turbines because of the additional mass introduced on the structure. Ice build-up is dangerous because it can reduce the generated power up to 25-50% of its design value, and the additional mass (up to 7-10% of the total mass) affects the dynamic behavior, causing excessive vibrations, higher bending moments, imbalance of the rotor, and noise (Corten and Veldkamp, 2001; Khalfallaha and Koliub, 2007; Bolton, 2007). Accumulation of dirt and bugs on the leading edge of the airfoil affects the aerodynamic efficiency of the airfoil by up to 20% of its design value, and is particularly critical for offshore towers (and towers operating in sandy environments) so much that the cleaning of the blades is recommended every few weeks (Ibsen and Liingaard, 2006; Andersen *et al.*, 2008) and their operational life is reduced to half of their design length with respect to ground-based towers. The initial clean model of the wind turbine, therefore, does not satisfactorily represent the actual behavior of the system.

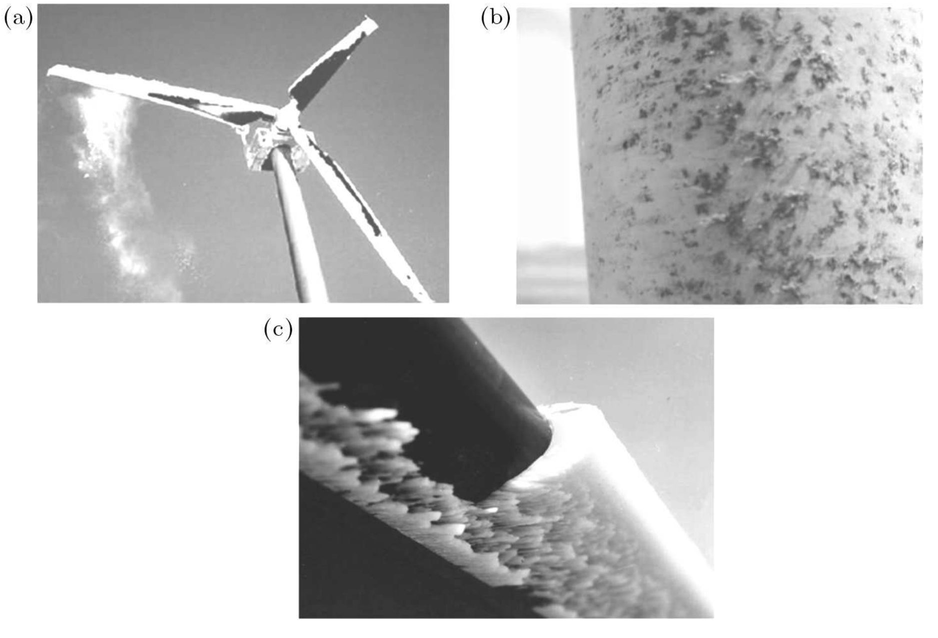

Fig. 1. Examples of the effect of ice and bugs on wind-turbine and rotorcraft blades; (a) ice on wind turbine, (b) bugs on wind turbine, (c) ice on helicopter blade

Rotorcraft operations are also greatly affected by icing accretion (Fig. 1c). Unlike aircraft propellers, helicopter blades collect ice along the entire leading edge of the airfoil at temperatures below 10°C causing an increase in drag (Palacios *et al.*, 2008; Coffman, 1987), flow separation and high vibration levels due both to uneven ice adhesion and progressive ice shedding from the blade due to centrifugal and aerodynamic forces (Gent *et al.*, 2000). One of the consequences of this behavior is that the maximum available power of the engine can be reached before the generation of the required torque to sustain the required operation.

Moreover, damage detection systems of the helicopter main rotor are still not generally available because of their high cost and complexity. Limited rotor system fault detection is provided as part of usage monitoring as well as automatic rotor track and balance systems. A comprehensive Health and Usage Monitoring System (HUMS) should provide post-flight diagnostic capabilities through the processing of flight data at ground stations in order to improve the detection of structural degradations. The focus of this paper is on vibration monitoring during operations as a means to achieve condition based maintenance (Stevens, 2001). In-flight or post-flight data processing requires simple and fast procedures for model updating so that changes in the system can be rapidly detected and analyzed.

The goal of the proposed approach, called *Property Identification Algorithm*, is to update the properties of a numerical model to achieve accurate predictions of the dynamic response of the system. This result is achieved by "tuning" a numerical model so that it accurately predicts the actual behavior of the system in every part of its life based on a limited amount of isolated measurement points so that the response at non-measured locations can be accurately predicted. The use of experimental measurements to identify and update the dynamical properties of a finite element model is known as model updating, and it has been extensively applied to structural dynamic in Friswell and Mottershead (1995) and Mottershead and Friswell (1993). The Property Identification Algorithm, however, does not focus on the accurate extrapolation of the changes in physical properties but is based on the Confluence Approach presented in McColl *et al.* (2010), Chierichetti *et al.* (2010, 2011). The approach presented in these papers computes corrections to the external loads in order to improve the prediction of the dynamic response, and it assumes accurate knowledge of the physical properties of the system, based on very few measurements of the response. Similar to the Confluence Algorithm, the proposed approach improves the dynamic response of a periodic system through a fast and simple updating technique. In contrast, the Property Identification Algorithm achieves this objective by updating the physical properties of the system and assuming accurate knowledge of the external loads. This assumption requires either having an *a priori* accurate model of the loads or achieving an accurate prediction of the loads through the Load Confluence Algorithm.

The proposed approach is ideally suited to the monitoring of the response of periodic systems such as wind-turbines and helicopters. It requires only the measurement of the dynamic response of the system and therefore allows modal identification under operations and in situations where the structure is difficult to excite by externally applied forces, Brincker *et al.* (2003). The predicted response of an initial model of the system is combined to reference data for the definition of simple algebraic relations between the corrections of mass and stiffness distributions and the difference between the measured and numerical responses, as discussed in Section 2. In Section 3, the potentialities of the algorithm are demonstrated through numerical validation in the case of a simple lumped-parameters system for variations in mass, and/or stiffness.

2. Property Identification Algorithm

The goal of the Property Identification Algorithm is the mapping of the response of a modified system through the identification of changes in dynamic properties (natural frequencies and modes). The application to rotating environments admits the assumption that the applied loads, and as a consequence the dynamic response, vary periodically with time and can be expanded through a Fourier series.

2.1. Concept

The Property Identification Algorithm consists of an initial numerical model of the structure, a set of experimental measurements at a limited number of locations, and a procedure that estimates the difference in dynamic properties between the numerical model and the experimental measurements. A block-diagram representation of the component of the procedure is depicted in Fig. 2. The applied loads are assumed to be known.

The dynamic model of the structure is defined by a mass matrix $\mathbf{M}$ and a stiffness matrix $\mathbf{K}$, the set of available experimental measurements is denoted as $\boldsymbol{e}_E(\boldsymbol{x})$, where $\boldsymbol{x}$ is a vector defining the location of the sensors, and array $\boldsymbol{e}_N(\boldsymbol{x})$ stores the numerical response. The following notation is used throughout the paper: bold, lower case defines vectors, bold, upper case defines matrices.

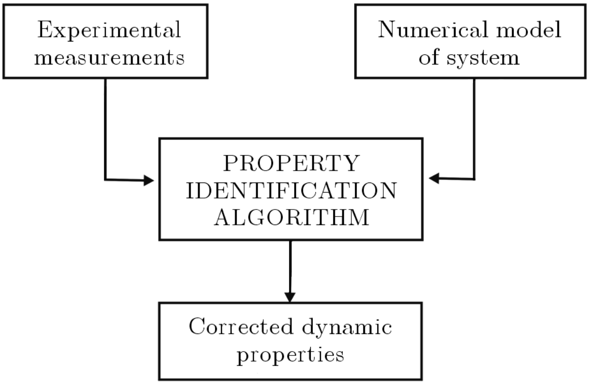

Fig. 2. Schematic of the Property Identification Algorithm

The procedure can be summarized as the following sequence of steps:

- A numerical model of the system is built from an initial guess of the physical properties of the system.
- The solution of the initial model estimates the dynamic response $\boldsymbol{e}_N(\boldsymbol{x})$ at the sensors location $\boldsymbol{x}$.
- The numerical and measured responses are compared and the error vector $\Delta\boldsymbol{e} = \boldsymbol{e}_E - \boldsymbol{e}_N$ is calculated.
- Corrections for the mass and/or stiffness matrices are calculated based on $\Delta\boldsymbol{e}$ through a formulation of the problem in the modal domain, as described in Section 2.2.
- A modified set of dynamic properties is found from the solution to the new eigenvalue problem with the updated mass and stiffness matrices.

2.2. Modal procedure for property estimation

Structural degradation can occur in a system as a change in stiffness, or mass, or mass and stiffness distributions. Three different procedures have been developed to analyze each of these problems separately.

2.2.1. Change in stiffness

Consider a general undamped linear system

$$\mathbf{M}\ddot{\boldsymbol{u}}(t) + \mathbf{K}\boldsymbol{u}(t) = \boldsymbol{F}(t) \tag{2.1}$$

where array $\boldsymbol{u}(t)$ stores the N degrees of freedom of the solution, and $\boldsymbol{F}(t)$ is the array of the generalized applied loads. This system (defined as "initial" system) is characterized by natural frequencies $\boldsymbol{\omega}$ and modes $\mathbf{P}$.

The real model (defined as "reference") of the system is

$$\widehat{\mathbf{M}}\ddot{\widehat{\boldsymbol{u}}} + \widehat{\mathbf{K}}\widehat{\boldsymbol{u}} = \boldsymbol{F}(t) \tag{2.2}$$

It is assumed that the applied loads are accurately modeled and that the reference system undergoes the same loading condition as the initial system. The reference model is characterized by natural frequencies $\widehat{\boldsymbol{\omega}}$ and modes $\widehat{\mathbf{P}}$. Suppose an inaccuracy exists in the estimation of the stiffness matrix, therefore

$$\widehat{\mathbf{M}} = \mathbf{M} \qquad\qquad \widehat{\mathbf{K}} = \mathbf{K} - \Delta\mathbf{K} \tag{2.3}$$

with $\Delta\mathbf{K}$ unknown. The eigenvectors of the modified system $\widehat{\mathbf{P}}$ are assumed to be a linear combination of the initial modes $\mathbf{P}$ through a matrix $\boldsymbol{\alpha}$ of coefficients

$$\widehat{\mathbf{P}} = \mathbf{P}\boldsymbol{\alpha} \tag{2.4}$$

The difference between Eq. (2.1) and (2.2) leads to

$$\mathbf{M}(\ddot{\boldsymbol{u}} - \ddot{\widehat{\boldsymbol{u}}}) + \mathbf{K}(\boldsymbol{u} - \widehat{\boldsymbol{u}}) - \Delta\mathbf{K}\widehat{\boldsymbol{u}} = \mathbf{0} \tag{2.5}$$

with $\boldsymbol{u} = \mathbf{P}\boldsymbol{q}$ and $\widehat{\boldsymbol{u}} = \widehat{\mathbf{P}}\widehat{\boldsymbol{q}} = \mathbf{P}\boldsymbol{\alpha}\widehat{\boldsymbol{q}}$. The difference in generalized modal coordinates is defined as

$$\overline{\Delta\boldsymbol{z}} = \boldsymbol{q} - \boldsymbol{\alpha}\widehat{\boldsymbol{q}} \tag{2.6}$$

Therefore the difference in the dynamic response is defined as $\boldsymbol{u} - \widehat{\boldsymbol{u}} = \mathbf{P}\overline{\Delta\boldsymbol{z}}$. Pre-multipling Eq. (2.5) by $\mathbf{P}^\top$, and defining the projection of the change in the stiffness matrix in the modal domain as $\boldsymbol{\mathcal{K}} = \mathbf{P}^\top\Delta\mathbf{K}\mathbf{P}$, Eq. (2.5) results

$$\mathbf{I}\overline{\Delta\ddot{\boldsymbol{z}}} + \operatorname{diag}(\omega_i^2)\overline{\Delta\boldsymbol{z}} + \boldsymbol{\mathcal{K}}\boldsymbol{\alpha}\widehat{\boldsymbol{q}} = \mathbf{0} \tag{2.7}$$

The response of the system and the generalized coordinates can be related through a matrix $\mathbf{B}$ and its pseudo-inverse as:

— numerical response

$$\boldsymbol{e}_N(x,t) = \mathbf{B}(x)\boldsymbol{q}(t) \tag{2.8}$$

— experimental measurement

$$\boldsymbol{e}_E(x,t) = \widehat{\mathbf{B}}(x)\widehat{\boldsymbol{q}}(t) \tag{2.9}$$

The definition of $\mathbf{B}$ depends on the reference quantities. In the case of experimental measurements, it depends on the type of sensors. For example, if e_i represents a displacement measurement at the location (x_i, y_i), B_{ij} represents the contribute of the modal displacement j at the location i. If strain gages are considered, B_{ij} represents the contribute of modal strain j at location i. A reduced number of modes m can be used in the analysis, that has to be lower than the number of sensors used to identify the response. Moreover, only modes that can be identified by the choice of sensors can be included.

Assume that the relation between matrices $\mathbf{B}$ and $\widehat{\mathbf{B}}$ is the same as the relation between $\mathbf{P}$ and $\widehat{\mathbf{P}}$, so that $\widehat{\mathbf{B}} = \mathbf{B}\boldsymbol{\alpha}$. This assumption is valid in a linear or linearized framework. The difference between the initial response and the reference signal is

$$\boldsymbol{e}_N - \boldsymbol{e}_E = \mathbf{B}(\boldsymbol{q} - \boldsymbol{\alpha}\widehat{\boldsymbol{q}}) = \mathbf{B}\overline{\Delta\boldsymbol{z}} \tag{2.10}$$

and

$$\overline{\Delta\boldsymbol{z}} = \mathbf{B}^{+}\Delta\boldsymbol{e} \tag{2.11}$$

Equation (2.7) thus becomes

$$\mathbf{B}^{+}\Delta\ddot{\boldsymbol{e}} + \operatorname{diag}(\omega_i^2)\mathbf{B}^{+}\Delta\boldsymbol{e} + \boldsymbol{\mathcal{K}}\mathbf{B}^{+}\widehat{\boldsymbol{e}} = \mathbf{0} \tag{2.12}$$

The externally applied loads are supposed to be periodic as well as the response of the system, and can be expanded in a Fourier series of frequency Ω

$$\Delta\boldsymbol{e} = \Delta\boldsymbol{e}_0 + \sum_{j=1}^{M}[\boldsymbol{e}_{c_j}\cos(j\Omega t) + \boldsymbol{e}_{s_j}\sin(j\Omega t)] \tag{2.13}$$

The harmonic balance of Eq. (2.12) leads to

$$\begin{aligned}
&\operatorname{diag}(\omega_i^2)\mathbf{B}^{+}\Delta\boldsymbol{e}_0 + \boldsymbol{\mathcal{K}}\mathbf{B}^{+}\widehat{\boldsymbol{e}}_0 = \mathbf{0}\\
&\operatorname{diag}(-j^2\Omega^2 + \omega_i^2)\mathbf{B}^{+}\Delta\boldsymbol{e}_{c_j} + \boldsymbol{\mathcal{K}}\mathbf{B}^{+}\widehat{\boldsymbol{e}}_{c_j} = \mathbf{0}\\
&\operatorname{diag}(-j^2\Omega^2 + \omega_i^2)\mathbf{B}^{+}\Delta\boldsymbol{e}_{s_j} + \boldsymbol{\mathcal{K}}\mathbf{B}^{+}\widehat{\boldsymbol{e}}_{s_j} = \mathbf{0}
\end{aligned} \tag{2.14}$$

The unknown of the system is the change in the stiffness matrix in the modal domain $\boldsymbol{\mathcal{K}}$. Assume that it is possible to approximate $\Delta\mathbf{K}$ with a rank-1 approximation (see Appendix A for details) such that

$$\widehat{\mathbf{K}} = \mathbf{K} - \Delta\mathbf{K} = \mathbf{K} - \boldsymbol{h}\boldsymbol{h}^{\top} \tag{2.15}$$

and

$$\boldsymbol{\mathcal{K}} = \mathbf{P}^{\top}\Delta\mathbf{K}\mathbf{P} = \mathbf{P}^{\top}\boldsymbol{h}\boldsymbol{h}^{\top}\mathbf{P} = \boldsymbol{\beta}\boldsymbol{\beta}^{\top} \tag{2.16}$$

Eq. (2.14) becomes

$$\begin{aligned}
&\operatorname{diag}(\omega_i^2)\mathbf{B}^{+}\Delta\boldsymbol{e}_0 + \boldsymbol{\beta}\boldsymbol{\beta}^{\top}\mathbf{B}^{+}\widehat{\boldsymbol{e}}_0 = \mathbf{0}\\
&\operatorname{diag}(-j^2\Omega^2 + \omega_i^2)\mathbf{B}^{+}\Delta\boldsymbol{e}_{c_j} + \boldsymbol{\beta}\boldsymbol{\beta}^{\top}\mathbf{B}^{+}\widehat{\boldsymbol{e}}_{c_j} = \mathbf{0}\\
&\operatorname{diag}(-j^2\Omega^2 + \omega_i^2)\mathbf{B}^{+}\Delta\boldsymbol{e}_{s_j} + \boldsymbol{\beta}\boldsymbol{\beta}^{\top}\mathbf{B}^{+}\widehat{\boldsymbol{e}}_{s_j} = \mathbf{0}
\end{aligned} \tag{2.17}$$

These non-linear system of equations is solved with a Newton-Raphson iterative method.

2.2.2. Change in mass

The change in dynamical properties due to a modification in the mass distribution of the system is analogous to the previously described procedure. The differences between the two cases are underlined in the following. The reference system is in this case characterized by an unknown change in the mass matrix such that

$$\widehat{\mathbf{M}} = \mathbf{M} - \Delta\mathbf{M} \qquad\qquad \widehat{\mathbf{K}} = \mathbf{K} \tag{2.18}$$

The aim is in this case to reconstruct the difference in mass $\Delta\mathbf{M}$ from the observation of the response of the reference system at a limited number of points, and to improve the prediction of the initial system. The difference between Eq. (2.1) and (2.2), considering Eq. (2.18), leads to

$$\mathbf{M}(\ddot{\boldsymbol{u}} + \ddot{\widehat{\boldsymbol{u}}}) + \mathbf{K}(\boldsymbol{u} - \widehat{\boldsymbol{u}}) - \Delta\mathbf{M}\ddot{\widehat{\boldsymbol{u}}} = \mathbf{0} \tag{2.19}$$

The change in the mass matrix projected in the modal domain is defined as $\boldsymbol{\mathcal{M}} = \mathbf{P}^\top\Delta\mathbf{M}\mathbf{P}$ and it is approximated as a rank-1 matrix (Appendix A) such that

$$\widehat{\mathbf{M}} = \mathbf{M} - \Delta\mathbf{M} = \mathbf{M} - \boldsymbol{g}\boldsymbol{g}^\top \tag{2.20}$$

and

$$\boldsymbol{\mathcal{M}} = \mathbf{P}^\top\Delta\mathbf{M}\mathbf{P} = \mathbf{P}^\top\boldsymbol{g}\boldsymbol{g}^\top\mathbf{P} = \boldsymbol{\eta}\boldsymbol{\eta}^\top \tag{2.21}$$

A modal expansion of Eq. (2.19) leads to

$$\mathbf{I}\overline{\Delta\ddot{\boldsymbol{z}}} + \operatorname{diag}(\omega_i^2)\overline{\Delta\boldsymbol{z}} + \boldsymbol{\mathcal{M}}\boldsymbol{\alpha}\ddot{\widehat{\boldsymbol{q}}} = \mathbf{0} \tag{2.22}$$

that becomes

$$\mathbf{I}\mathbf{B}^+\Delta\ddot{\boldsymbol{e}} + \operatorname{diag}(\omega_i^2)\mathbf{B}^+\Delta\boldsymbol{e} + \boldsymbol{\mathcal{M}}\mathbf{B}^+\ddot{\widehat{\boldsymbol{e}}} = \mathbf{0} \tag{2.23}$$

with the introduction of the previously defined matrix $\mathbf{B}$. The same hypothesis on the periodic nature of the external load is assumed. A Fourier expansion of all quantities and harmonic balance of Eq. (2.23) lead to

$$\begin{aligned}
&\operatorname{diag}(\omega_i^2)\mathbf{B}^+\Delta\boldsymbol{e}_0 = \mathbf{0}\\
&\operatorname{diag}\Big(1 - \frac{\omega_i^2}{j^2\Omega^2}\Big)\mathbf{B}^+\Delta\boldsymbol{e}_{c_j} + \boldsymbol{\mathcal{M}}\mathbf{B}^+\widehat{\boldsymbol{e}}_{c_j} = \mathbf{0}\\
&\operatorname{diag}\Big(1 - \frac{\omega_i^2}{j^2\Omega^2}\Big)\mathbf{B}^+\Delta\boldsymbol{e}_{s_j} + \boldsymbol{\mathcal{M}}\mathbf{B}^+\widehat{\boldsymbol{e}}_{s_j} = \mathbf{0}
\end{aligned} \tag{2.24}$$

The first equation on the zeroth coefficient is generally verified in itself and only the other two equations will be brought forward. Introducing the rank-1 approximation of the modal mass matrix $\boldsymbol{\mathcal{M}}$, the solution to the non-linear problem can be found through the Newton-Raphson procedure.

2.2.3. Change in mass and stiffness

The previous procedures can be combined and generalized in a unique algorithm in the case of a contemporaneous change in the mass and stiffness matrices. It is therefore assumed that the reference system is characterized by unknown modifications in the mass and stiffness distribution so that

$$\widehat{\mathbf{M}} = \mathbf{M} - \Delta\mathbf{M} \qquad\qquad \widehat{\mathbf{K}} = \mathbf{K} - \Delta\mathbf{K} \tag{2.25}$$

Following the same steps as previously described, the non-linear system of equations in the frequency domain is

$$\begin{aligned}
&\mathrm{diag}\,(\omega_i^2)\mathbf{B}^+\Delta\boldsymbol{e}_0 - \boldsymbol{\beta}\boldsymbol{\beta}^\top\mathbf{B}^+\widehat{\boldsymbol{e}}_0 = \mathbf{0}\\
&\mathrm{diag}\,(-j^2\Omega^2 + \omega_i^2)\mathbf{B}^+\Delta\boldsymbol{e}_{c_j} - \boldsymbol{\beta}\boldsymbol{\beta}^\top\mathbf{B}^+\widehat{\boldsymbol{e}}_{c_j} + j^2\Omega^2\boldsymbol{\eta}\boldsymbol{\eta}^\top\mathbf{B}^+\widehat{\boldsymbol{e}}_{c_j} = \mathbf{0}\\
&\mathrm{diag}\,(-j^2\Omega^2 + \omega_i^2)\mathbf{B}^+\Delta\boldsymbol{e}_{s_j} - \boldsymbol{\beta}\boldsymbol{\beta}^\top\mathbf{B}^+\widehat{\boldsymbol{e}}_{s_j} + j^2\Omega^2\boldsymbol{\beta}\boldsymbol{\beta}^\top\mathbf{B}^+\widehat{\boldsymbol{e}}_{s_j} = \mathbf{0}
\end{aligned} \tag{2.26}$$

and can be solved with the Newton-Raphson iterative method.

3. Numerical validation

3.1. Concept

The approach used for the numerical validation of the algorithm is described in this section. The initial model of the system is known, and its dynamic response is calculated in a particular loading, and labeled as "initial". Known structural modifications either in the mass and stiffness distribution (or both) are then added to the initial model, and its dynamic response is computed in the same loading condition and stored as "reference". The use of a numerically generated reference response is due to the lack of experimental measurements.

The corrections to the initial mass and stiffness matrices are then found by comparison of the initial and reference response. The response of the updated system is called "final". The characteristics of the algorithm are assessed by comparing the final and reference responses, and the identified changes in mass and stiffness with the real, known modifications introduced in the reference model.

3.2. Results

The algorithm is validated by the analysis of a 14 degrees of freedom lumped-parameter system (Fig. 3). A concentrated periodic load is applied at degree of freedom 10, with excitation frequencies of 4.5 rad/s and 9 rad/s. The natural frequencies of the initial system are enumerated in Table 1.

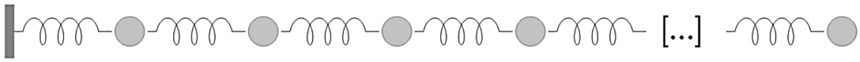

Fig. 3. Schematic of a lumped-parameters mass-spring system.

Table 1. Natural frequencies of the initial model

mode	ω_i [rad/s]
1	3.56
2	10.01
3	16.45
4	23.39
5	28.82
6	32.68

The ability of the algorithm to capture structural modifications both in the mass and stiffness distribution is investigated, as specified in Table 2.

Table 2. Description of the analyzed cases

ID	modes	control points	modification
1	1:14	1:14	$k_3 = 108.5\,\mathrm{N/m}$
2	1:3	1,4,7,10,13	$k_3 = 108.5\,\mathrm{N/m}$
3	1:6	1,3,5,7,9,11,13	$k_3 = 108.5\,\mathrm{N/m}$
4	1:6	1,3,5,7,9,11,13	$k_3 = 90\,\mathrm{N/m}$, $k_5 = 15\,\mathrm{N/m}$, $k_9 = 75\,\mathrm{N/m}$
5	1:3	1,4,7,10,13	$m_3 = 0.15\,\mathrm{kg}$
6	1:6	1,3,5,7,9,11,13	$m_3 = 0.05\,\mathrm{kg}$, $k_3 = 90\,\mathrm{N/m}$
7	1:6	1,3,5,7,9,11,13	$m_3 = 0.05\,\mathrm{kg}$, $k_3 = 90\,\mathrm{N/m}$ with noise

The main factors that influence the ability of the approach to converge to the exact solution are the number of modes in the modal expansion and the choice of control points (both total number and location). Their influence is investigated in this section as well as the influence of noise in the reference signals.

Initially, a change in stiffness at degree of freedom 3 is introduced. A complete modal expansion and a complete set of control points are considered in Case 1 to ensure that the algorithm exactly captures the modifications of the system when a complete modal expansion is used. However, when a lower number of modes and control points is considered, as for example in Case 2 (three modes and five control points), the modifications in natural frequencies (Table 3) and eigenvectors (Figs. 4) are captured with an accuracy of 1% on the modes included in the modal expansion, while the change in stiffness cannot be captured. This behavior is due to the use of a truncated modal expansion that causes the stiffness matrix to lose its original structure: in fact, both the initial and reference systems are characterized by a tridiagonal, sparse stiffness matrix, while the final stiffness matrix loses its sparse characteristic. The deformed shape of the system at a specified time instant, Fig. 5, reveals that even if the change in stiffness is not accurately captured, the dynamic response is greatly improved with only three modes to represent the dynamic response. Before the application of the Property Identification Algorithm, the mean error with respect to the reference system is about 30%, while after the application of the algorithm is reduced to 3%.

Table 3. Case 2. Initial and final error between the reference (ω_r), the initial and the identified (ω_f) natural frequencies

ID	ω_r [rad/s]	ω_f [rad/s]	E_{in} [%]	E_{fin} [%]
1	3.86	3.86	−7.7	0.02
2	10.55	10.63	−5.1	0.8
3	16.46	16.49	−0.1	0.2
4	23.84	23.39	−1.9	−1.9
5	30.12	28.82	−4.3	−4.3
6	39.46	32.68	−17.2	−17.2

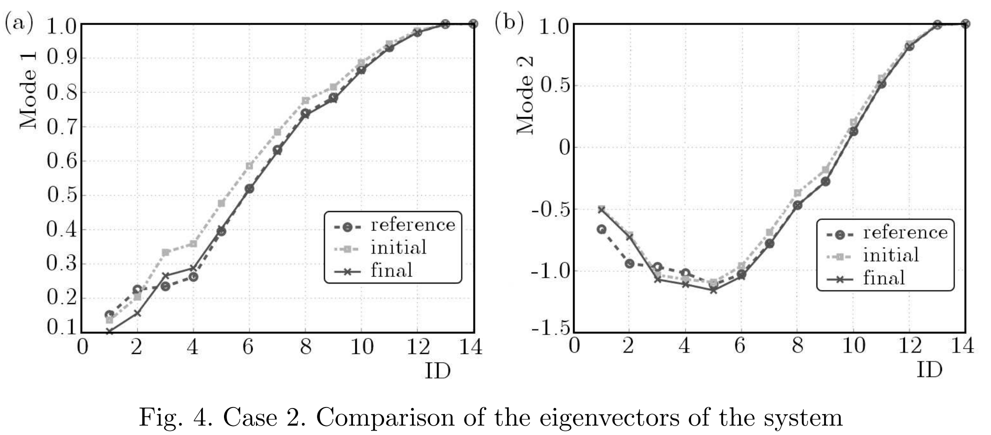

Fig. 4. Case 2. Comparison of the eigenvectors of the system

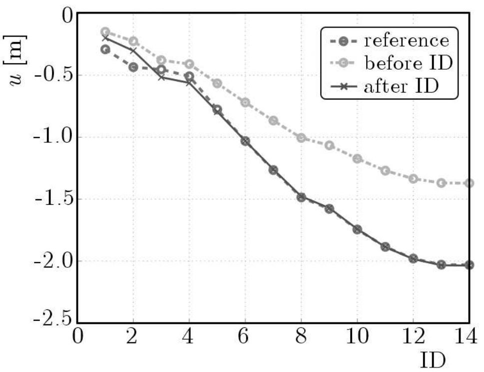

Fig. 5. Case 2. Deformed shape of the system

The inclusion of three higher modes and two control points (Case 3) highly improves the prediction of the modal properties, both of the natural frequencies and of the eigenvectors. The errors on higher frequencies, such as the 5th and 6th natural frequency, are reduced to about 1% as the lower frequencies. However, the algorithm still encounters difficulties in the physical representation of the change in stiffness. The dynamic response of the system is accurately represented with a mean error of about 4%, as shown in Fig. 6.

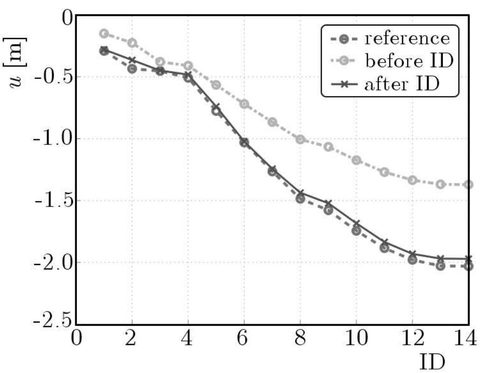

Fig. 6. Case 3. Deformed shape of the system

The presence of multiple modifications in the system is analyzed in Case 4 and represents a critical condition for the algorithm. As described in Section 2.2, in fact, the change in the characteristic matrices is modeled as a rank-1 matrix approximation, which corresponds to an elementary modification of the system. Also in this case, the algorithm is able to improve the natural frequencies of the system, but cannot accurately update the stiffness distribution. However, the time history of the system at different degrees of freedom is identified with an accuracy of about 5% (initial error of about 50%), as illustrated by Figs. 7 and 8. The dynamic response is effectively mapped, both at degrees of freedom used as control points (Fig. 7a) and not used by the identification approach (Fig. 7b). A broader view of the behavior of the whole system is given by the analysis of the deformed shape at a particular time instant (Fig. 8), and it confirms the exceptional improvements achieved in the prediction of the final response of the whole system.

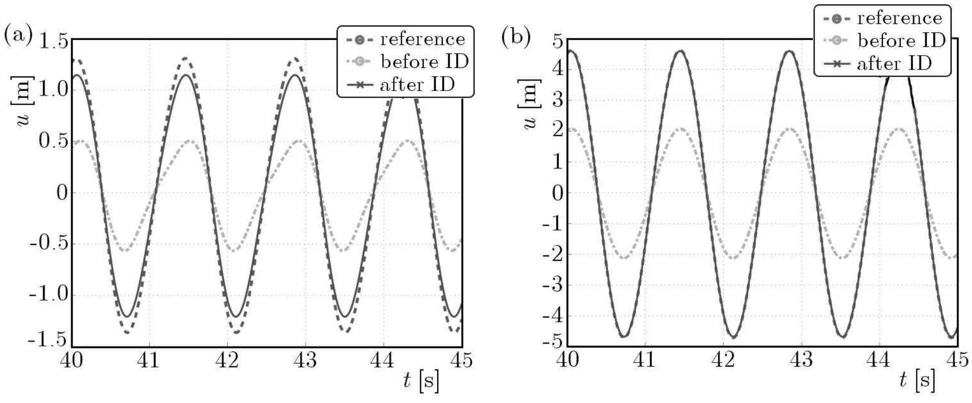

Fig. 7. Case 4. Time history at different degrees of freedom; (a) DOF 2 – not control point, (b) DOF 11 – control point

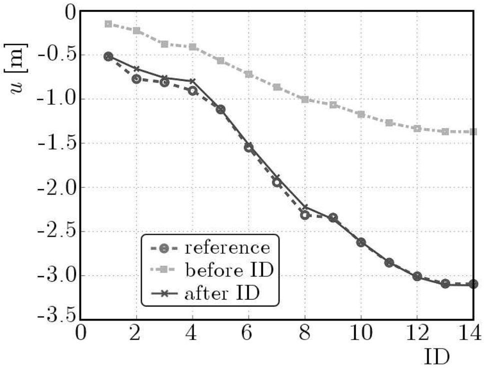

Fig. 8. Case 4. Deformed shape of the system

A change in the mass distribution at degree of freedom 3 is introduced in Case 5. This analysis represents a parallel problem for Case 2, and the behavior of the identification procedure is very similar. The natural frequencies and the lowest eigenvectors are identified with an accuracy of about 3%. As previously underlined, the change in physical mass is not properly captured due to the incompleteness of the modal expansion. The dynamic response is accurately identified in the whole system, both at control points, Fig. 9b, and at points not considered as the reference, Fig. 9a. The analysis of the deformed shape of the system confirms this observation (Fig. 10).

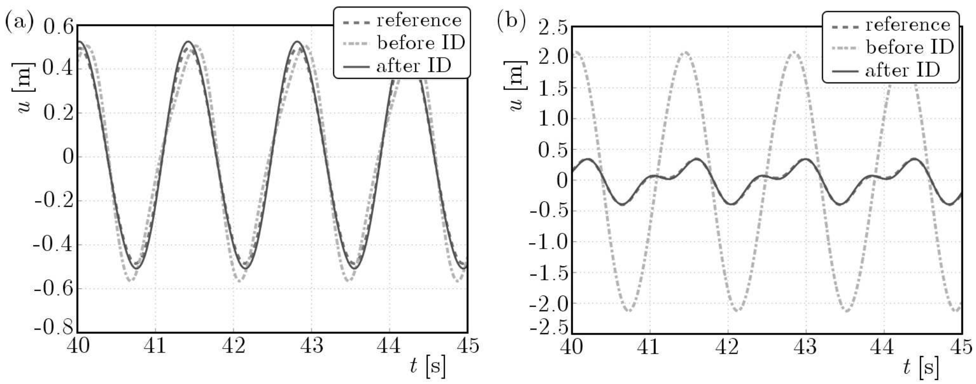

Fig. 9. Case 5. Time history at different degrees of freedom; (a) DOF 2 – not control point, (b) DOF 11 – control point

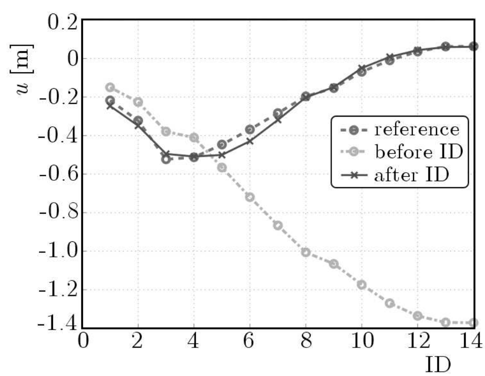

Fig. 10. Case 5. Deformed shape of the system

Finally, simultaneous changes in the mass and stiffness distributions are considered. In Case 6, six modes and seven reference points are considered in the identification of the dynamic response.

As noticed in the previous sections, the algorithm can capture major modifications in modal properties with an incomplete modal expansion within an accuracy of 10% (Table 4), while the mass and stiffness distributions maintain large inaccuracies: the algorithm cannot distinguish between changes in mass and stiffness. Figures 11 and 12 reveal that the dynamic response of the system is accurately identified within an error of 5% at critical locations.

Table 4. Case 6. Initial and final error between the reference (ω_r), the initial and the identified (ω_f) natural frequencies

ID	ω_r [rad/s]	ω_f [rad/s]	E_{in} [%]	E_{fin} [%]
1	3.77	3.77	−5.5	0.1
2	8.51	8.51	17.6	0.05
3	14.93	14.92	10.2	−0.1
4	22.84	22.44	2.4	−1.8
5	29.81	29.58	−3.3	−0.8
6	39.37	35.37	−17.0	−10.2

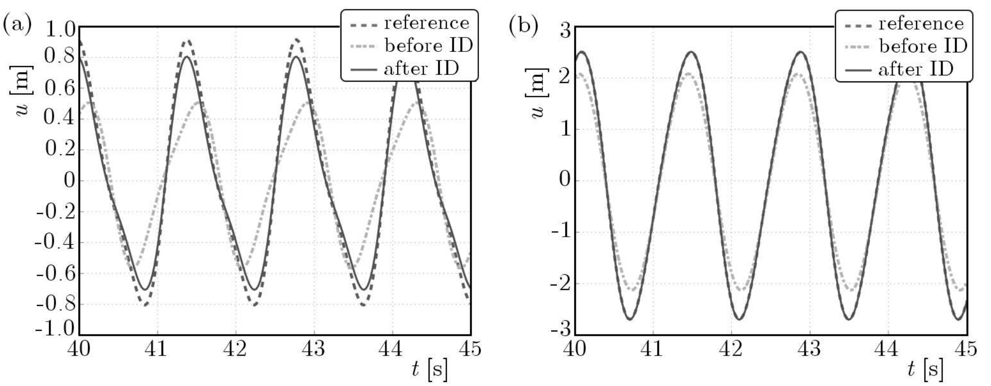

Fig. 11. Case 6. Time history at different degrees of freedom; (a) DOF 2 – not control point, (b) DOF 11 – control point

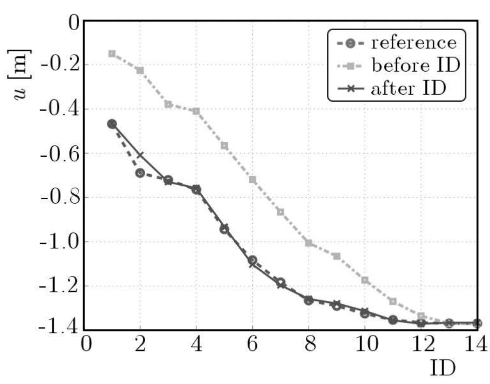

Fig. 12. Case 6. Deformed shape of the system

The noise contained in the reference signals is an important factor for the convergence of the algorithm. Random noise has been added to the reference response characterized by lower signal levels (DOF: 1,2,3,4). The noise level is about 5% the amplitude of the considered signal. The results of the identification procedure are shown in Figs. 13 and 14. The mean error on the deformed shape is reduced from about 25% before the application of the Property Identification Algorithm to less than 10% after the identification, and the error on the natural frequencies is reduced from a maximum of 17% to 1.5%.

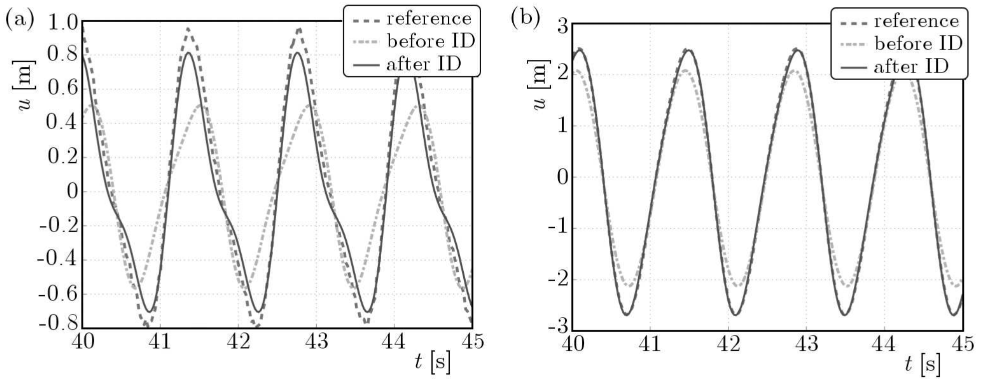

Fig. 13. Case 7. Time history at different degrees of freedom; (a) DOF 2 – not control point, (b) DOF 11 – control point

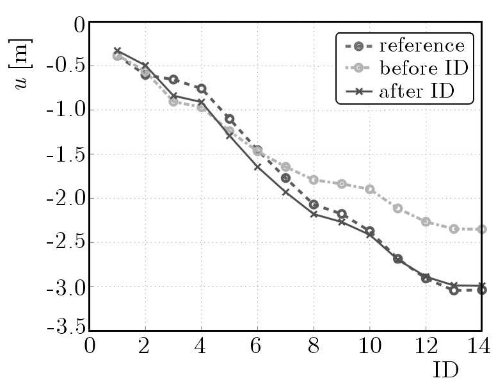

Fig. 14. Case 7. Deformed shape of the system

It is therefore demonstrated that the algorithm is effectively capable of extracting information on the complete map of the response from a minimal set of reference/experimental data, and to improve the predictions of both the response and modal properties of the initial model in the presence of structural degradations, even in the presence of noise in the signals. These results are promising for applications in more complex environments.

4. Conclusion

An innovative approach for the mapping of the response in the presence of structural modifications has been formulated, which integrates minimal experimental data into the initial and inaccurate model of a system. Simple validation cases demonstrate that the algorithm is capable of mapping the response of the system in the complete domain, based on discrete reference data of the dynamic response. The procedure identifies the presence of changes in the mass and stiffness distribution and updates the modal properties of the system to best represent the reference dynamic properties.

A. Rank-1 tensor approximation

A rank-1 tensor is the simplest possible tensor, and is defined as

$$A_1 = \boldsymbol{u}\boldsymbol{w}^\top \tag{A.1}$$

where $\boldsymbol{u}$ and $\boldsymbol{w}$ are column vectors. In general, a tensor can always be expressed as a linear combination of r rank-1 tensors, where r is the rank of the tensor.

In the case of a dynamic system, a rank-1 approximation of the updated mass and stiffness matrices corresponds to an elementary modification of the system. For example, in the case of a three-degrees-of-freedom, lumped-parameter system

$$\begin{aligned} \mathbf{K} &= \begin{bmatrix} k_1+k_2 & -k_2 & 0 \\ -k_2 & k_2+k_3 & -k_3 \\ 0 & -k_3 & k_3 \end{bmatrix} \\ \mathbf{M} &= \operatorname{diag}([m_1, m_2, m_3]) \end{aligned} \tag{A.2}$$

If m_2 and k_2 are reduced by Δm and Δk respectively, the changes in the mass and stiffness matrices are in fact

$$\Delta\mathbf{K} = \begin{bmatrix} \Delta k & -\Delta k & 0 \\ -\Delta k & \Delta k & 0 \\ 0 & 0 & 0 \end{bmatrix} = \Delta k \begin{bmatrix} 1 \\ -1 \\ 0 \end{bmatrix} \begin{bmatrix} 1 & -1 & 0 \end{bmatrix}$$

$$\Delta\mathbf{M} = \operatorname{diag}([0, \Delta m, 0]) = \Delta m \begin{bmatrix} 0 \\ 1 \\ 0 \end{bmatrix} \begin{bmatrix} 0 & 1 & 0 \end{bmatrix} \tag{A.3}$$

References

1. Andersen P., Brincker R., Ventura C., Cantieni R., 2008, Modal estimation of civil structures subject to ambient and harmonic excitation, *Proc. XXVI IMAC*, Orlando, Florida, February 4-7

2. Bolton R., 2007, *Assessment of the Sound Level Study for the Mars Hill Wind Farm*, http://www.rapid-response-consulting.com/userfiles/file/noiseassessment.pdf

3. Brincker R., Ventura C.,Andersen P., 2003, Why output-only modal testing is a desiderable toll for a wide range of practical applications, *Proc. XXI IMAC*, Orlando, Florida, February 3-6

4. Chierichetti M., McColl C., Palmer D., Bauchau O., Ruzzene M., 2010, Analytical and experimental approaches to rotor components stress predictions, *The 1st Joint International Conference on Multibody System Dynamics*, Lappeenranta, Finland, May 25-27

5. Chierichetti M., Ruzzene M., Bauchau O., Palmer D., McColl C., 2011, Prediction of UH-60A blade loads: an insight on Confluence Algorithm to correct internally generated airloads, *Proceedings of the 67th American Helicopter Society Forum*, Virginia Beach, May 3-5

6. Coffman H.J. Jr., 1987, Helicopter rotor icing protection methods, *Journal of the American Helicopter Society*, **32**

7. Corten G.P., Veldkamp H.F., 2001, Insects can halve wind-turbine power, *NATURE*, brief communications, **412**, 42-43

8. Friswell M.I., Mottershead J.E., 1995, *Finite Element Model Updating in Structural Dynamics*, Kluwer Academic Publishers

9. Gent R.W., Dart N.P., Cansdale J.T., 2000, Aircraft icing, *Philosophical Transactions of the Royal Society. A. Mathematical, physical and engineering sciences*, **358**, 2873-2911

10. Ibsen L.B., Liingaard M., 2006, Prototype bucket foundation for wind turbines natural frequency estimation, DCE Technical Report, 9, Aalborg University

11. Khalfallaha M.G., Koliub M.A., 2007, Effect of dust on the performance of wind turbines, *Desalination*, **209**, 209-220

12. McColl C., Palmer D., Chierichetti M., Bauchau O., Ruzzene M., 2010, Comprehensive UH - 60 loads model validation, *Proceedings of the 66th American Helicopter Society Forum*, Phoenix, Arizona, May 11-13

13. Mottershead J.E., Friswell M.I., 1993, Model updating in structural dynamics: A survey, *Journal of the Sound and Vibration*, **167**, 347-375

14. Palacios J.L, Smith E.C., Rose J.L., 2008, Investigation of an ultrasonic ice protection system for helicopter rotor blades, *Proc. American Helicopter Society 64th Annual Forum*, Montreal, Canada, April 29 - May 1

15. Stevens P., 2001, Active interrogation of helicopter main rotor faults using trailing edge flap actuation, Phd. dissertation

16. Wallace J.Jr., Dawson M., *O&M for wind turbine blades*, www.renewableenergyfocus.com/view/3243

Udoskonalanie modeli w dynamice konstrukcji za pomocą algorytmu konfluencji

streszczenie

Identyfikacja dynamicznej odpowiedzi konstrukcji wykazującej cechy degradacji strukturalnej ma praktyczne zastosowanie w układach monitorowania stanu i może przyczynić się do poprawy bezpieczeństwa lotu śmigłowców oraz zwiększenia efektywności pracy turbin wiatrowych przy jednoczesnym obniżeniu kosztów eksploatacji. W pracy przedstawiono tzw. Algorytm Identyfikacji Właściwości (*Property Identification Algorithm*) będący kombinacją numerycznej i eksperymentalnej procedury, której celem jest udoskonalenie modelu przy ograniczonym zbiorze danych doświadczalnych do precyzyjnego przewidywania dynamicznej odpowiedzi układu z degradacją strukturalną. Algorytm oparto na dekompozycji modalnej i dyskretnych pomiarów eksperymentalnych oraz sformułowano dla przypadku wymuszeń harmonicznych. Wykazano, że odpowiedzi dynamiczne modelu udoskonalonego pozwala na uzyskanie dokładnej mapy rzeczywistych odpowiedzi w zadanym obszarze parametrów. W artykule opisano zaproponowany algorytm i przedstawiono kilka przykładów jego weryfikacji.

Manuscript received March 1, 2011; accepted for print April 29, 2011